European Journal of
Nuclear
Medicine

Review article

# Nitroimidazoles and imaging hypoxia

Adrian Nunn*, Karen Linder*, H. William Strauss**,

Bristol-Myers Squibb Pharmaceutical Research Institute, Princeton, N.J., USA

**Abstract.** Decreased tissue oxygen tension is a component of many diseases. Although hypoxia can be secondary to a low inspired $pO_2$ or a variety of lung disorders, the commonest cause is ischemia due to an oxygen demand greater than the local oxygen supply. In tumors, low tissue $pO_2$ is often observed, most often due to a blood supply inadequate to meet the tumor's demands. Hypoxic tumor tissue is associated with increased resistance to therapy. In the heart tissue hypoxia is often observed in persistent low-flow states, such as hibernating myocardium. In patients with stroke, hypoxia has been associated with the penumbral region, where an intervention could preserve function. Despite the potential importance of oxygen levels in tissue, difficulty in making this measurement in vivo has limited its role in clinical decision making. A class of compounds known to undergo different intracellular metabolism depending on the availability of oxygen in tissue, the nitroimidazoles, have been advocated for imaging hypoxic tissue. When a nitroimidazole enters a viable cell the molecule undergoes a single electron reduction, to form a potentially reactive species. In the presence of normal oxygen levels the molecule is immediately reoxidized. This futile shuttling takes place for some time, before the molecule diffuses out of the cell. In hypoxic tissue the low oxygen concentration is not able to effectively compete to reoxidize the molecule and further reduction appears to take place, culminating in the association of the reduced nitroimidazole with various intracellular components. The association is not irreversible, since these agents clear from hypoxic tissue over time. Initial development of nitroimidazoles for in vivo imaging used radiohalogenated derivatives of misonidazole, such as fluoromisonidazole, some of which have recently been employed in patients. Two major problems with fluoromisonidazole are its relatively low concentration within the lesion and the need to wait several hours to permit clearance of the agent from the normoxic background tissue (contrast between lesion and background typically <2:1 at about 90 min after injection). Even with high-resolution positron emission tomographic imaging, this combination of circumstances makes successful evaluation of hypoxic lesions a challenge. Single-photon agents, with their longer half-lives and comparable biological properties, offer a greater opportunity for successful imaging. In 1992 technetium-99m labeled nitroimidazoles were described that seem to have at least comparable in vivo characteristics. Laboratory studies have demonstrated preferential binding of these agents to hypoxic tissue in the myocardium, in the brain, and in tumors. These investigations indicate that imaging can provide direct evidence of tissue with low oxygen levels that is viable. In the experimental setting this information is useful to plan a more aggressive approach to treating tumors, or revascularize a heart suffering ischemic dysfunction. Even from this early vantage point the utility of measuring tissue oxygen levels with external imaging suggests that hypoxia imaging could play a major role in clinical decision making.

**Key words:** Nitroimidazoles – Hypoxia – Heart – Brain – Tumors

**Eur J Nucl Med (1995) 22:265–280**

## Introduction

All mammalian tissues require a supply of oxygen to meet their metabolic demands. For intracellular metabolism to take place, surprisingly low levels of oxygen, intracellular pressures of 3–5 mm of oxygen, are sufficient [1]. This low intracellular concentration is the result of oxygen delivery by diffusion from the capillary to the intracellular environment. Perfusion of tissue with blood flow beyond its demand (luxury perfusion) is a waste of cardiac work, while inadequate oxygen supplies limit the ability of intracellular metabolism to meet the cell's energy needs. As oxygen supplies are reduced, maximum output decreases, and systems are downregulated to maintain viability. For short periods (seconds), cellular work can exceed the oxygen supply, but an oxygen debt occurs that must be repaid [2]. If the debt becomes too large, cellular integrity is threatened. As a result, normal tissue has an extensive network of mechanisms to provide tight coupling between the tissue's requirements for oxygen and the amount delivered to the tissue [3]. Many

* *Present address:* Bracco Research USA, Rt 206 and Provinceline Road, Princeton, NJ 08543, USA

*Correspondence to:* H.W. Strauss at his present address: Division of Nuclear Medicine, Stanford University School of Medicine, Room HO101, Stanford, CA 94305, USA

diseases alter the supply-demand relationship. Atherosclerotic disease, for example, reduces the ability of the vessel to dilate and physically narrows vessels, initially limiting the supply of blood that can be delivered to the tissue during peak demand, and in severe cases, in the basal state. In tumors, the increased cell mass requires additional oxygen supplies to keep the cells alive. To meet this demand tumors produce a number of factors to promote the growth of new vessels into the lesion. Often, however, the increased demand for oxygen outstrips the supply, rendering a portion of the tumor mass hypoxic. Under these circumstances, a measurement of perfusion does not adequately characterize the tissue. A direct indicator of oxygen tension in the tissue would be useful.

Potential markers that could be used to estimate tissue oxygen levels include perfusion, acidosis (due to lactate production in ischemic tissue), or a direct marker of decreased intracellular $pO_2$ (hypoxia). Perfusion imaging identifies the relative delivery of oxygen at the cellular level. In the brain the regional distribution of technetium-99m hexamethylpropylene amine oxime (HMPAO) and $^{99m}$Tc-ethyl cysteinate dimer (ECD) can identify areas of low flow, but cannot differentiate between scar and ischemia. In the myocardium, thallium clearance from tissue is influenced to some degree by ischemia. However, about one-third of patients with myocardial ischemia do not have redistribution [4], suggesting that other parameters also play a significant role. Under circumstances of persistent low flow rest/redistribution imaging with thallium may be helpful in defining ischemia, but its true sensitivity is difficult to assess.

One measure of an initial supply/demand mismatch is a reduction in intracellular pH. The primary factor controlling intracellular pH is the tissue concentration of $CO_2$, which averages 50 mmHg [5]. In addition to ischemia, increased work can transiently increase tissue $CO_2$. In normal tissue local perfusion responds to this acidosis with vasodilatation and increased perfusion. The highly soluble $CO_2$ is then removed by this increased flow, restoring normal pH. Tissue that is acutely, irreversibly damaged, paradoxically, has an elevated pH, typically above 7.5. Although positron emission tomographic (PET) techniques have been developed to measure intracellular pH [6], the procedures are complex and difficult to perform as a routine examination. An additional problem with this technique is that tumors have a highly variable blood flow, and frequently have a wide range of intracellular pH [7].

Tissue oxygenation is a common denominator to the cellular energy equation [8]. The delivery of oxygen is a major limiting factor controlling cellular performance. Oxygen has minimal solubility in extracellular fluid, but must diffuse from red cells in the capillary to the mitochondria in the cell. Although the delivery of oxygen to tissue has sufficient excess capacity to compensate for a wide range of demand, a marked deficiency of intracellular oxygen results in immediate reduction in function and prolonged hypoxia [9] is a prevalent cause of irreversible injury in all mammalian tissues. These considerations suggest that a marker of decreased intracellular oxygen tension would be an effective indicator of tissue that is viable and dysfunctional in any organ.

In 1955 Nakamura discovered that a 5-nitroimidazole (azomycin) was active against infections associated with anaerobic conditions [10]. Over the intervening 40 years many nitroimidazole analogs have been synthesized, leading to antibiotics such as metronidazole, tinidazole, nimorazole, and ornidazole which are effective against bacteria and protozoa that thrive in a hypoxic environment [11]. This unique behavior of nitroimidazoles in a low oxygen environment led to investigations of their utility as hypoxic tissue sensitizers, to increase the response of hypoxic tissue to radiation or chemical therapy [12]. The idea that such compounds might be adapted to allow the visualization of hypoxic tissue in vivo has been discussed for more than 10 years [13]; however, it is only relatively recently that practical application of the idea has occurred.

## Mechanisms

Nitroimidazoles are reduced intracellularly in all cells, but in the absence of adequate supplies of oxygen, they undergo further reduction to more reactive products that bind to cell components [11]. The formation of these products is initiated by an enzyme-mediated single-electron reduction of the nitro group to a free radical which is an anion at neutral pH. The reduction pathway can proceed in successive steps past the hydroxylamine derivative to terminate at the relatively inactive amine derivative (Fig. 1).

The compound enters cells by diffusion, with the lipophilicity of the molecule as a major determinant of its penetration into the intracellular environment. The enzyme responsible for the initial single-electron reduction is the pyruvate: ferredoxin oxidoreductase complex in anaerobic organisms. A specific enzyme responsible for this reduction in mammalian cells has not been identified, but several enzymes are capable of reducing nitroimidazoles [14]. Xanthine oxidase, an enzyme found in many mammalian cells, is often used [15] as a test system in laboratory studies.

All anaerobes have redox potentials of about –430 to –460 mV, which is typical for ferredoxin, whereas the most negative redox potential in aerobes are those of the NAD/NADH and NADP/NADPH couples at about –320 mV. The 5-nitroimidazole metronidazole (METRO) has a reduction potential of –415 mV and is efficiently reduced in anaerobes but not in aerobes [11]. Thus the 5-

$$RNO_2 \xrightarrow{1e} \dot{R}NO_2^- \xrightarrow{1e} RNO_2 \xrightarrow{2e} RNOH \xrightarrow{2e} RNH_2$$

**Fig. 1.** Proposed multistep reduction pathway for nitroimidazoles in the cell

nitroimidazoles show activity against Gram-positive and Gram-negative bacteria and protozoa. In order to achieve useful reduction in aerobes the reduction potential of the nitroimidazole group must be reduced. This is done by changing the substitution pattern from the 5-nitro of METRO to the 2-nitro of misonidazole (MISO), which has a reduction potential of –389 mV [12].

The initial reduction to the free radical anion is reversed by intracellular oxygen because oxygen (reduction potential of –155 mV) has a higher electron affinity than the nitro group. The rate of oxidation is dependent on the intracellular concentration of oxygen. Thus the initial step in the pathway gives the reaction its oxygen sensitivity. Subsequent steps provide the retention that is necessary to differentiate normoxic from hypoxic tissue by imaging. Reduction occurs in all tissue with viable enzymatic processes but retention only occurs in those tissues with low oxygen tension because reoxidation of the original compound is slowed, permitting additional reductive reactions to take place. These reactions are shown in Fig. 2.

Kedderris et al. [14] suggest that the free radical nitro anion does not react with DNA or sulfhydryl-containing compounds such as glutathione but is primarily a biologically unreactive intermediate. The actual reactive products from the biological reduction of nitroimidazoles have not been isolated but hydroxylamine derivatives have chemical reactivities similar to those of the purported reactive products [18].

The cellular components that the reduced products react with have not been unequivocally identified. METRO reacts slightly with sulfhydryl-containing cytoplasmic proteins and possibly with DNA although no actual METRO-DNA adducts have been isolated from cells. Kedderris and Miwa [14] explored the binding of reduced METRO with pure DNA or proteins in vitro and found only about 1.2% or 0.03% binding respectively, suggesting that this is not the major trapping mechanism. Similarly, the target for MISO and other 2-nitroimidazole radiosensitizers is generally thought to be DNA but there is much debate on the mechanisms involved. A MISO-glutathione adduct has been detected in cells [20]. From the point of view of transient trapping of an imaging agent, covalent binding to macromolecules is not necessary (and unlikely). Formation of less permeable species, such as the amine, which is charged, is sufficient.

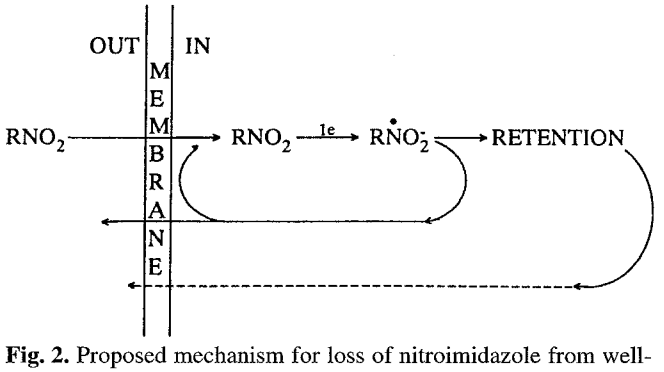


**Fig. 2.** Proposed mechanism for loss of nitroimidazole from well-oxygenated tissue

## Characteristics of MISO and other radiosensitizers

MISO and its analogs have been the major agents investigated thus far. The potency of the nitroimidazoles as radiosensitizers in vitro is related to their reduction potential [21], but not their lipophilicity. Unfortunately, as the reduction potential is increased, the stability of the compound decreases. Experience has demonstrated that reduction potentials close to that of MISO are necessary for these agents to work. A parallel effort has been directed towards reducing lipophilicity, to minimize the peripheral and central neuropathies associated with high doses, while maintaining tumor uptake [22, 23].

### *Pharmacology*

Use of MISO as a radiosensitizer requires high doses, which can saturate metabolic and excretory mechanisms. At high doses (~0.5 g/m$^2$ per day) MISO is toxic to hypoxic cells in the absence of radiation (with or without additional chemotherapeutic agents) [12]. When MISO is used at pharmacologic doses, it is metabolized by the liver, with less than 20% of the dose appearing unchanged in the urine. The major metabolites are the O-demethylated derivative (DEMISO) and glucuronide conjugates. O-demethylation is not possible with fluoromisonidazole or iodovinylmisonidazole, which do not contain the methoxy group, and so one should expect a different pattern of metabolism with these compounds. There is an inverse correlation between lipophilicity and the amount of drug excreted unchanged in the urine because the more lipophilic drugs are extracted and metabolized by the liver. Similarly, protein binding for MISO is negligible but increases up to about 50% for the more lipophilic derivatives such as benznidazole [21].

After injection of pharmacologic quantities of MISO, 0.5–1mmol/kg, the blood clearance is biphasic, with ~30% of the dose clearing with a half-life of about 30 min and the remainder clearing with a half-life of 70–90 min [22, 23]. Compounds with lipophilicity equal to or greater than MISO have a 3- to 12-fold longer second component of clearance as the dose administered is increased from 0.5 to 5 mmol/kg [21]. This is a direct result of the saturation of the metabolizing enzymes for the more lipophilic compounds. The lowest of these doses exceeds the normal *radiosensitizer* dose of MISO and is orders of magnitude greater than doses used for imaging studies. This makes the interpretation of the high-dose toxicity tests very difficult and raises questions about the relevance of these data to the assessment of toxicity when radiopharmaceutical doses are used.

Workman and Brown [21] found no difference in the clearance kinetics and extent of metabolism of nitroimidazoles in several mammalian species (making the mouse a reasonable predictor for behavior in man).

*Oxygen sensitivity*

A number of different units have been used for reporting oxygen concentration. The most common units are %, ppm, and Torr (≡ mmHg=$pO_2$). Conversion rates are: room air =20.5% $O_2$=205 000 ppm=156 Torr. Normal tissue oxygen values have been measured in animals respiring room air using a variety of methods [28]. Using microelectrodes the extracellular fluid around specific cells can be sampled. Using this technique, the dog left ventricular endocardium had a $pO_2$ of 14–17 and the epicardium a $pO_2$ of 27–31; the cat brain cortical gray matter measured 19–40 Torr while the white matter ranged from 6 to 16 Torr [28]. Values in cells can only be inferred, for example, using the saturation of myoglobin measured spectrophotometrically. Using this method the dog gracilis muscle at rest averaged 17 Torr, while muscle working at 95% of maximum oxygen consumption averaged 1.5 Torr.

The oxygen concentration at which the nitroimidazoles are retained is usually reported as the $K_m$, that is the oxygen concentration at which the retention/activity is 50% of anoxic-normoxic value (this $K_m$ is similar to but should not be confused with the $K_m$ used to characterize enzymatic reactions). The $K_m$ is independent of MISO concentration at imaging doses but varies with concentration at radiosensitizer and chemical sensitizer doses (see above). In general the $K_m$ for radiosensitization is about 2000–5000 ppm $O_2$ 500 ppm $O_2$ for chemosensitization, and 200 ppm $O_2$ for toxicity [25].

A range of $K_m$ values for binding or radiosensitization have been obtained for MISO in a variety of tumor cell lines, including human melanoma cells, and in normal tissues (Table 1).

Investigators initially used autoradiography to evaluate localization of MISO in various tissues:

1. *Tumors.* Chapman et al. [13] exposed spheroids of Chinese hamster V79 tumor cells to carbon-14 labeled MISO for 3 h and then autoradiographed sections taken after extensive washing. Spheroids of <0.15 mm in diameter did not contain appreciable amounts of radioactivity but spheroids of >0.6 mm in diameter contained a ring of radioactivity lying just outside the central necrotic core (caused by insufficient oxygen due to extraction of oxygen by the outermost cells). The ring of MISO deposition represents the layer of cells that have intact enzymes but which have an oxygen concentration which is unable to effectively deoxidize the initial reduction product. Similar rings of MISO deposition were found in tumors in animals and in man where deposition of radioactivity in subcutaneous tumors increased with the distance of the tumor cells from blood vessels [26, 27].

2. *Ischemic brain tissue.* In a stroke model, Hoffman et al. [28] demonstrated increased MISO radioactivity in the ischemic hemisphere within 2–7 h after injection. The concentration increased with the severity of the stroke. When flow decreased to <25% of the normal hemisphere, radioactivity was retained.

3. *Heart.* Garrecht and Chapman [29] used autoradiographs to evaluate mice pretreated with isoproterenol to induce myocardial ischemia and observed about twice as much MISO retention in the myocardium of treated animals compared to controls.

**Table 1.** $K_m$ of MISO in tumor cells and normal tissue

| Cells | $K_m$ $O_2$ (ppm) | Reference |
|---|---|---|
| V79 | 2000 | Franko [28a] |
| V79 | 5000 | Roizin-Towle et al. [29] |
| V79 (sandwich) | 2000 | Hlatky et al. [30] |
| Human tumors | 1000–6000 | Franko [28a] |
| Human tumors | 2000 | Urtasun et al. [31] |
| EMT-6 tumor | 3000 | Van Os-Corby et al. [31a] |
| Heart (mouse) | 2500 | Van Os-Corby et al. [31a] |
| Liver (mouse) | 3000 | Van Os-Corby et al. [31a] |
| Brain (mouse) | 4000 | Van Os-Corby et al. [31a] |

## Imaging

Extending these exciting experimental data to the realm of imaging in vivo requires that the tracer localize in zones of low flow in sufficient quantity to permit detection within an acceptable interval of time, and provide sufficient contrast between normal and ischemic tissue to enable detection of subtle decreases in tissue oxygen tension. The sensitivity of nitroimidazole imaging for the detection of hypoxic tissue will be determined by four factors:

– The amount of radiopharmaceutical delivered to the site of ischemia

– The fraction which gets past the initial reversible reaction

– The rapidity of clearance of radioactivity from normoxic cells

– Sufficient duration of retention in hypoxic cells to record high-quality images

The specificity of nitroimidazole imaging will depend on:

– The contrast between lesion and background

– The oxygen concentration at which trapping occurs

The following section describes the chemistry and rationale for compounds that have been synthesized and tested for imaging decreased tissue oxygen concentration in vivo. Structures of the compounds are shown in Figs. 3 and 4.

*Brominated MISO derivatives*

Brominated misonidazole, 4-bromomisonidazole (BrMISO) labeled with bromine-77 ($t_{1/2}$ = 57 h), was the first

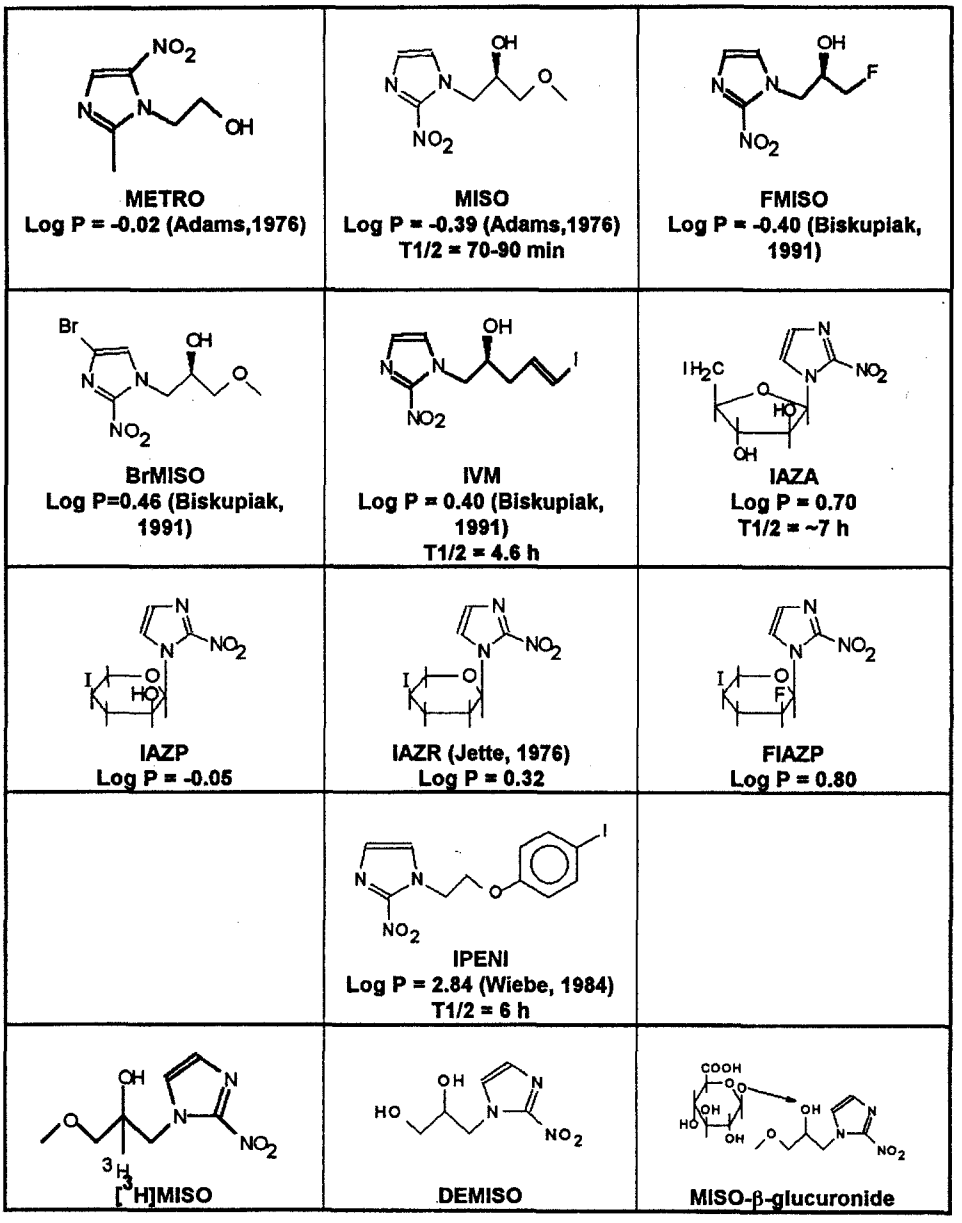


**Fig. 3.** Structures of selected compounds tested for imaging ($T_{1/2}$ values are for second phase of blood clearance)

MISO derivative to be labeled with a gamma-emitting radionuclide with a view to in vivo imaging. Bromine was chosen over iodine because of the greater strength of the bromine – carbon bond. The radionuclide is well suited to the presumed pharmacokinetics, based on those of MISO, which suggested that the best images of tumors would not be obtained for about 24 h after injection [13, 30].

Rasey et al. [31] and Jette et al. [32] used $Br_2$ as the labeling agent produced by exchange of molecular bromine with $NH_4{}^{82}Br$. Grunbaum et al. [23] obtained better results by generating the bromination agent in situ using anhydrous $K^{82}Br$ and *N*-chlorosuccinimide. Labeling with $Br_2$ produced lower specific activity material and final yields of <25% relative to the in situ method, which had yields of >75%. Part of the problem of the $Br_2$ reaction was the formation of the dibrominated product together with the 5-bromo derivative.

*Iodinated MISO derivatives*

An iodovinyl derivative of MISO, iodovinylmisonidazole (IVM), was developed by Biskupiak et al. [33] to take advantage of the stability of I–C bonds, reducing the likelihood of dehalogenation as observed with BrMISO. Another advantage of the iodovinyl group is the relative ease of radioiodination using the vinyltributylstannane precursor, which allows the production of IVM at no-carrier-added levels using high specific activity [$^{131}$I]NaI or [$^{123}$I]NaI. Starting with sodium iodide at 1280 Ci/mmol they obtained IVM in 50%–60% radio-

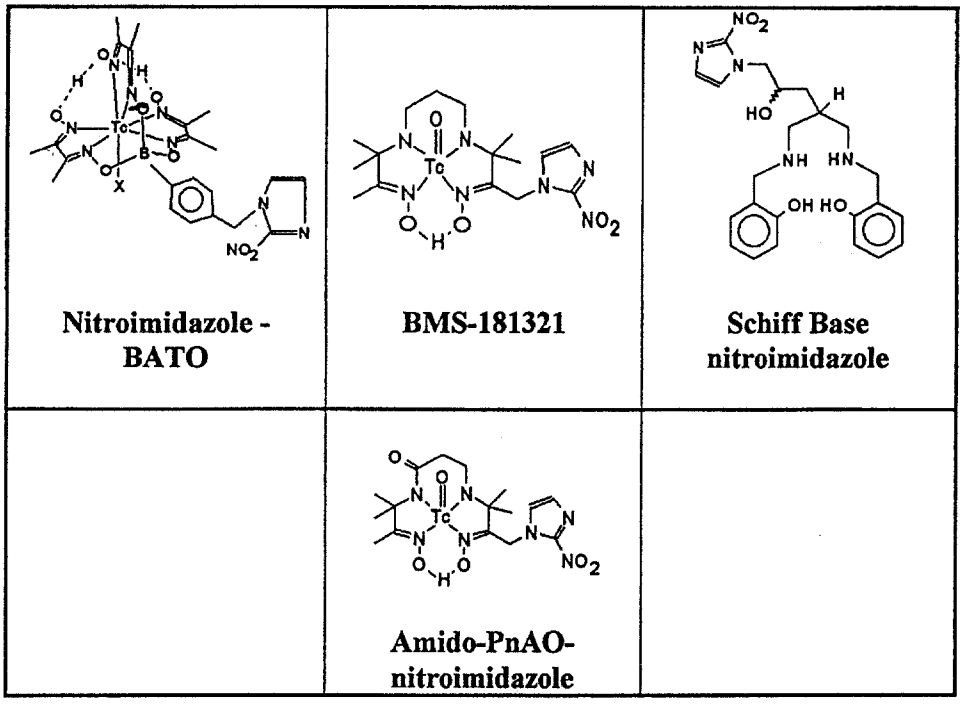


**Fig. 4.** Structures of selected technetium-containing nitroimidazoles tested for imaging

chemical yield, >98.5% radiochemical purity, with a specific activity of about 400 Ci/mmol after high-performance liquid chromatography (HPLC) purification.

After fluoromisonidazole and BrMISO, IVM is structurally the closest to MISO of all the nitroimidazoles developed for imaging purposes. The iodovinyl group replaces the methoxy group of the MISO and only requires an additional methylene group between it and the hydroxy derivatized carbon for stability. This raises the lipophilicity to that of the BrMISO, which is almost 10 times more lipophilic than MISO.

Wiebe et al. [34] examined an iodophenoxy derivative of PENI, a known radiosensitizer. The parent compound was iodinated using ICI to give both mono- (IPENI) and diiodinated (DIPENI) derivatives which were separated by HPLC. [$^{131}$I]IPENI was prepared by exchange with a radiochemical yield of about 90% at a specific activity of 200 mCi/mmol. The high lipophilicity of IPENI (log P=2.84), was reflected in 90% protein binding as measured by ultrafiltration, which in turn gave longer clearance times from the blood.

*Iodinated sugars with attached nitroimidazoles*

Jette et al. [35] iodinated azomycin riboside, a known radiosensitizer and sugar-containing homologue of MISO, in an effort to obtain a compound which was less lipophilic than IPENI. The resulting compound, IAZR, has a lipophilicity (log P=0.32) comparable to that of BrMISO and IVM. The iodination of azomycin riboside gave the IAZR in 70% yield as a colorless oil. This was exchange labeled using Na$^{125}$I in dimethylformamide at 84°C for 3 h or using the melt method in pivalic acid. The mixture was purified by reverse phase HPLC. Approximately 20% protein binding was seen by ultrafiltration, which is more than with MISO but less than with IPENI and entirely consistent with the lipophilicity. There was some deiodination.

A second sugar-containing MISO derivative is iodoazomycin arabinoside (IAZA), synthesized by Mannan et al. [36]. This is an isomer of IAZR. Exchange labeling was performed by heating in DMF at 70°C for 3.5 h to give material with a specific activity of 21 mCi/m*M* after preparative HPLC. Although no protein binding data are given, it is likely that the high lipophilicity (log P=0.70) of this isomer will result in increased protein binding and thus slower blood clearance. A third member of this class is IAZG, in which the pentose IAZR has been replaced by a hexose. Unfortunately, this compound suffered from deiodination, in similar fashion to IAZA. To reduce deiodination, the compound was further modified by moving the iodine closer to the ring, to make IAZP [37]. This agent has been tested in biodistribution studies, but still suffers from deiodination. Another member of this class is FIAP, in which one of the hydroxy groups was replaced with a fluorine [38]. This agent has the stronger iodine – carbon bond of IAZP (reflected in the necessity for direct iodination) and has lower thyroid activity in biodistribution studies. The substitution of the hydroxyl group by the fluorine changes the lipophilicity and hydrogen bonding attributes of the molecule. These factors will alter blood clearance and tissue uptake, but it is unclear whether they will alter retention in hypoxic tissues. The compound could be considered a cross-over between the PET compounds labeled with fluorine-18 and the single-photon agents labeled with $^{123}$I.

*Fluorinated MISO derivatives*

The synthesis of $^{18}$F-fluoromisonidazole via fluorination of 1-(2,3-epoxypropyl)-2-nitroimidazole [39] with TBAF and its biodistribution in rats [40] were first reported by the group at Washington University. The $^{18}$F-TBAF used for the fluorination was prepared by exchange labeling, so the specific activity of this material was relatively low. Grierson et al. [41] prepared the compound in 40% yield (EOB) with a specific activity of up to 670 Ci/mmol by reaction of the fluoroalkylating agent [$^{18}$F]epifluorohydrin with 2-nitroimidazole under basic conditions. This material, as well as the tritium-labeled analogue $^{3}$H-fluoromisonidazole, were used to study localization of the agents in hypoxic tumors [42, 43] and in a dog myocardial infarct model [44].

Although PET imaging with fluorinated misonidazole derivatives has demonstrated the principle of hypoxia imaging (see below), the limited contrast between normal and abnormal tissue and the need to wait about 90 min between injection and imaging limit the count rate, and hence images of limited quality are produced. The development of a technetium-based hypoxia imaging agent, with its longer physical half-life and more favorable dosimetry, would permit administration of higher doses and provide images of higher quality.

*Technetium derivatives*

The three classes of technetium compounds that have been studied are: (a) technetium BATO nitroimidazoles, (b) technetium PnAO and amido PnAO nitroimidazoles, and (c) the Schiff bases.

BATO analogues

The BATO analogues have the general formula of $TcX(dioxime)_3BR$ (X=Cl, OH; R=a nitroimidazole derivative; BATO=boronic acid adduct of technetium dioxime) [45]. These neutral molecules are formed in a template synthesis reaction between a nitroimidazole-bearing boronic acid derivative [46] and a technetium dioxime complex to form a seven-coordinate metal complex. These BATO nitroimidazoles were screened in an in vitro enzyme assay to determine whether these molecules would be recognized by the nitroreductase enzyme xanthine oxidase (XOD) as others have reported for misonidazole [47, 48] and fluoromisonidazole [49].

The nitroimidazole moiety on BATO nitroimidazole technetium complexes was enzymatically reduced in the absence of oxygen, demonstrating recognition by the enzyme [45], but the unchelated boronic acids and MISO were reduced at a much faster rate than the corresponding BATO complexes. These results suggested that the BATO nitroimidazoles have some of the characteristics required for a hypoxia imaging agent but that reduction in vivo could be slower than desired. However, the fact that BATO nitroimidazoles were recognized by XOD is of note, since few technetium-labeled compounds are recognized by enzymes.

The high lipophilicity of the BATOs relative to misonidazole and/or steric hindrance from the rather bulky Tc complex may hinder the binding of the nitro group at the active site of the enzyme and slow the reaction rate. An additional problem is the possible limitation of diffusion of the complex across cell membranes. These considerations led to the evaluation of other molecules which are known to carry technetium cores across membranes [51].

Screening studies were done in a blood-brain barrier model which used monolayers of bovine brain microvessel endothelial cells grown to confluence on aluminum oxide (Anocell) membranes. These cells form tight intercellular junctions and have few pinocytotic vesicles. The ability of test compounds to pass through the monolayer was measured relative to the permeability of $^{14}$C sucrose and $^{3}H$-$H_2O$ (controls for low and high permeability respectively).

The hypothesis that lipophilicity and high single-pass cerebral extraction imply high transendothelial permeability was not borne out by these studies. The BATO molecules had both high single-pass extraction and high lipophilicity values, but were found to have very low permeability through monolayers and a high degree of association with the cells. These results suggested that these lipophilic BATO nitroimidazoles may become trapped in the hydrophobic membrane, rather than entering the cytosol.

Technetium PnAO derivatives [50, 52]

The results with the BATO nitroimidazoles led us to screen other technetium cores. We found that $^{99m}$TcO(PnAO-1-(2-nitroimidazole)) [50] (called BMS-181321), a 2-nitroimidazole derivative of the well-known class of technetium(V) oxo propylene amine oxime (PnAO) complexes, was highly permeable through the bovine brain endothelial cell. The permeability of this molecule was about 60% that of water. Subsequent studies showed preferential localization of BMS-181321 in hypoxic brain, myocardium, and tumors [64, 66, 67, 71, 75, 79].

Under hypoxic conditions BMS-181321 was metabolized to a reduced polar species. Some of the metabolites were bound to protein, in keeping with literature postulates about the trapping mechanism of nitroimidazoles. However, the majority of the metabolites appeared to be low molecular weight polar products that did not pass readily from the cytosol into the extracellular medium. These results suggest that one of the trapping mechanisms for BMS-181321 in hypoxic cells is the formation of polar reduced metabolites that are preferably retained inside the cell due to lower permeability, rather than irreversible binding [53].

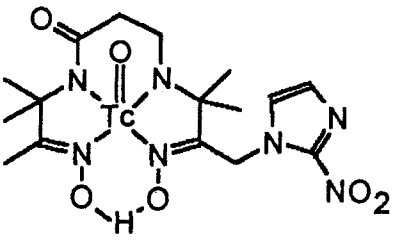

**Fig. 5.** Structure of the amido PnAO nitroimidazole described by Amersham International [61]

Technetium amido PnAO derivatives

An amido PnAO nitroimidazole (Fig. 5) was recently described by Amersham International [54]. The complex is formed by stannous reduction of $TcO_4$ in 40% yield, and HPLC purified to 80% yield.

Technetium Schiff base derivatives

Two other classes of technetium nitroimidazole compounds have been reported in the patent literature. The 6-substituted Schiff base nitroimidazole derivative, described by Neumeier et al. [55] was reported to give 2.8 times more activity bound to hypoxic Morris hepatoma 7777 tumor cell spheroids than to normoxic cells. Our studies with this compound [56] in cardiac myocytes under anoxic and hypoxic conditions revealed only minimal binding in hypoxic cells (38.2% of the activity bound to normoxic cells and 41.4% bound to hypoxic cells; anoxic to normoxic ratio of 1.08). The high degree of association with normoxic cells is consistent with results obtained in the permeability assay, where an appreciable amount of the complex was found to be associated with the membranes. A very low permeability index of –0.25 was obtained, indicating that, like the BATO nitroimidazoles, this Schiff base nitroimidazole does not readily cross cell membranes.

*The ideal agent*

The agents described above have a wide variety of lipophilicity, protein binding, and plasma clearance characteristics. It may be necessary to have several different agents to optimize visualization in cerebral ischemia, compared to myocardial ischemia or tumor hypoxia. An optimal agent should localize in the tissue of interest quickly, with a target/background ratio >3:1, and provide a sufficient photon flux to permit high-quality images to be recorded in a short time (at an acceptable radiation burden to the patient).

Ischemic tissue usually has decreased perfusion, limiting first-pass delivery of the tracer to the cells of interest. To optimize delivery, blood clearance should be relatively long compared to a perfusion agent [57]: a clearance half-time of several hours would be most suitable. In reality, however, it is preferable to detect ischemic/viable tissue as early as possible. Weighing these conflicting factors, a vascular half-life of ~10 min and a tenth-time of less than 45 min should provide adequate delivery while permitting imaging within an hour of injection.

Contrast is determined by the relative retention in ischemic tissue and clearance from normoxic tissue. Typically, although contrast increases over time, these agents appear to have some loss from the site of ischemic localization. In any total system, optimum images can be recorded at a time when a figure of merit optimizes the count rate and the ratio of lesion to adjacent tissue background. The biological characteristics of the radiopharmaceutical should be such that clearance from normal tissue parallels that of the blood. If delivery to ischemic tissue and clearance can be accomplished as desired, high-quality images could be recorded about 30 min after injection.

## Potential applications

*Heart*

To the extent that the criteria for an ideal agent are met, the agent should be useful in the evaluation of: (a) patients admitted to rule out myocardial infarction; (b) patients who, following thrombolytic therapy, have pain or ST changes that are slow to resolve; (c) individuals with markedly reduced contractile function possibly due to hibernating myocardium. Unfortunately, the known kinetics of delivery and nitroimidazole reduction make it less likely that the agent would be useful for the detection of transient ischemia.

The following vignette suggests a possible scenario where hypoxia imaging could be useful:

A 51-year-old man with a family history of coronary disease developed chest pain while showering after his morning exercise. The pain got worse while dressing, and became unrelenting on the way to the office. An EKG in the emergency room demonstrated marked ST segment elevation. Thrombolytic therapy was begun but chest pain and ST elevation persisted after the conclusion of infusion, in spite of morphine, infusion of nitroglycerin, and cautious administration of calcium channel blockers.

Since every minute counts, rapid identification of tissue at risk, e.g., areas with ischemic dysfunction that can be restored to normal function with restoration of perfusion, is needed. More than 1300 people die of myocardial infarction each day in the United States alone [58]. While the mortality has decreased remarkably as a result of improved treatment, optimal preservation of cardiac function requires restoration of perfusion to all viable tissue. After treating chest pain and arrhythmias and achieving hemodynamic stabilization, major management decisions concern the effectiveness of thrombolysis and whether additional mechanical intervention, such as

angioplasty or bypass surgery, is necessary. If reperfusion has been successful, or if the tissue is dead, further efforts to revascularize the tissue are unnecessary. On the other hand, if the tissue remains ischemic, additional intervention is warranted.

Under basal conditions the myocardium consumes the oxygen delivered by blood flowing at 8–10 ml $min^{-1}$ 100 $g^{-1}$ [59]. This increases to 30–40 ml $min^{-1}$ 100 $g^{-1}$ at peak exercise, for a dynamic range of three- to fourfold [60]. When the level of oxygen drops below ~50% of basal levels, myocardial work decreases. Further decreases cause the hypoxic myocardium to enter a quiescent state, where the cell maintains its "housekeeping" functions, awaiting the return of sufficient oxygenation to restore function. In the nonworking heart, oxygen required for cellular survival is ~1.5 ml $min^{-1}$ 100 $g^{-1}$ [61]. If the levels of oxygen in the cell decrease further, cell death occurs (probably due to an inability to adequately control intracellular calcium [62]). From a functional perspective, neither hypoxic nor dead myocardium contributes to the ejection of blood. Clinical management requires differentiation of these two conditions.

In this setting, there is a need for an imaging procedure to determine whether the tissue is still alive and at risk. The two currently available single-photon techniques, perfusion imaging or detecting acute necrosis, cannot reliably answer the questions. Perfusion imaging depicts the relative delivery of oxygen to the tissue. This measurement, while very useful, does not address whether that delivery is sufficient to meet the needs of the viable myocytes in that territory. This is particularly true in areas of nontransmural infarction.

A necrosis marker would not provide the answer in a patient with acute infarction for two reasons. First, most of the markers currently available require intervals of at least hours between the time of onset of necrosis and the time a positive scan can be obtained [63]. Second, even if perfusion is restored very rapidly, the patient is likely to have sustained some necrosis, making the scan positive but not defining whether viable but ischemic tissue is also present.

An imaging technique that specifically identifies viable but dysfunctional tissue is needed. The agent must localize and provide high-contrast images within minutes of injection to be useful for critical clinical decision making. The following summarizes the current state of information available with nitroimidazole-based imaging agents in the heart.

## Myocytes

Studies in isolated cardiac myocytes allow determination of uptake of putative hypoxia imaging agents under carefully controlled oxygen levels, in the absence of confounding factors such as blood flow that may affect distribution. Biskupiak et al. [33] compared the retention of fluoromisonidazole (FMISO) and IVM in separated adult rat myocytes. After 1 h IVM had an anoxic to normoxic ratio of 9.6. By 3 h this had risen to 22.0 and was similar to that of FMISO (20.3).

The behavior of $^{3}$H-FMISO has been compared to that of $^{131}$I-IVM, the technetium nitroimidazole complex BMS-181321 and congeners, as well as a Tc-PnAO nonnitro control (Table 2) [64]. Data obtained indicated that in vitro, retention in both normoxic and anoxic cells is dependent, in part, on the lipophilicity of the complexes. As log k' rose, the absolute uptake in both normoxic and hypoxic cells increased. $^{3}$H-fluoromisonidazole, the least lipophilic compound tested (log k'= –0.7), had the lowest level of uptake, 3% in normoxic cells and 8% in hypoxic cells, while BMS-181321, the most lipophilic compound tested, had retention of 22% and 50% respectively after a 1-h incubation. Uptake in normoxic cells plateaued within 1 min, suggesting that this activity was nonspecifically bound, rather than metabolically trapped. In contrast, activity levels in hypoxic myocytes rose over a 60-min period.

## Isolated perfused hearts

Shelton et al. [65] determined the retention of $^{18}$F-misonidazole in hypoxic, ischemic, and normal hearts and hearts subjected to ischemia and reperfusion prior to injection. They found about 200% greater retention in the

**Table 2.** Behavior of various nitroimidazole compounds and a nonnitroimidazole control in cardiac myocytes (from [69])

| Compound | Log k' | Normoxic cells at 60 min (%) | Hypoxic cells at 60 min (%) | H/N ratio |
|---|---|---|---|---|
| $^{3}$H-fluoromisonidazole | –0.7 | 3 | 8 | 2.6 |
| Tc-PnAO-6-amide-(2-nitro-imidazole) | –0.45 | 10 | 18 | 1.8 |
| $^{131}$I-Iodovinylmisonidazole | –0.19 | 12 | 26 | 2.2 |
| Tc-PnAO-1-(4-nitroimidazole) | 0.16 | 23 | 40 | 1.7 |
| Tc-PnAO-1-(2-nitroimidazole) | 0.31 | 22 | 50 | 2.3 |
| Control[a]: > Tc-PnAO-6-Me(nonnitro) | 0.31 | 17.4 | 22.7 | 1.3 |

[a] The data for the nonnitroimidazole control Tc-PnAO-6-Me demonstrate that the nitroimidazole moiety is required for selective retention in hypoxic cardiac myocytes

hypoxic and ischemic hearts compared to the controls and the ischemic/reperfused hearts. Even under these optimized circumstances, nonischemic tissue retained ~20% of the initially administered tracer. While ischemic hearts had a longer retention time, and the ischemic/normal tissue ratio with this agent was borderline for imaging, these investigators demonstrated the feasibility of imaging with this agent in a series of five dogs with experimental ischemia.

BMS-181321 retention in isolated rat hearts perfused with Krebs-Henseleit buffer was 2.5 times higher under hypoxic than under normoxic conditions [66]. The second phase of clearance of activity (retained after 2 min) had a $T_{1/2}$ of 170±30 min in normoxic hearts, whereas the hearts perfused with hypoxic buffer had a clearance $T_{1/2}$ of 604±112 min. In normoxic hearts, only 33% of the peak activity remained after 40 min of clearance. In contrast, 65% of the peak activity was retained in the hypoxic hearts.

When oxygen levels in perfusate were reduced from 544 to 29 Torr in graded intervals, each decrease in perfusate $pO_2$ caused a linear increase in the level of BMS-181321 retention, and a very strong correlation between the level of retention of BMS-181321 and the cytosolic [lactate]/[pyruvate] ratio was seen [67].

Kusuoka et al. [68] also studied the retention of BMS-181321 in isolated perfused rat heart under normoxic, hypoxic, or no-flow ischemia, followed by reperfusion. Under normoxic conditions, BMS-181321 was injected, and then allowed to wash out of the heart. After 10 min, absolute retention in the heart was <1% ID/g wet wt. In contrast, when hypoxic buffer was used at similar flow rates, retention in the heart at 10 min was 4 times higher.

## Experimental studies in vivo

The retention of IVM in the myocardium of dogs after partial LAD stenosis with or without demand ischemia was examined by Martin et al. [69]. Increased retention of radioactivity was seen in areas with reduced blood supply. Retention increased linearly as the blood flow in the tissue decreased below 30% of the baseline value. These areas of increased retention were shown by sonomicrometry to consist of viable tissue as there was a return of contractile function with relief of ischemia. This counters some of the criticisms of Goldstein [70] that hypoxia-localizing agents have not been shown to predict return of function. Additional studies demonstrated retention of IVM in animals with a severe stenosis and ischemia due to increased demand. Maximal ischemic tissue to blood ratios in the myocardium were 3.2 at 4 h post injection. Unfortunately, this work did not include attempts to obtain images of the myocardium.

BMS-181321 was coinjected with either $^{14}$C-deoxyglucose or $^{14}$C-misonidazole in rabbits 20 min after ligation of the left anterior descending artery (LAD) [71]. Double-label autoradiography revealed a similarity in the microregional distribution of the three agents in the border zone of the ischemic LAD territory. In contrast, a nonnitroimidazole control (Tc-PnAO-6-methyl) gave uniformly low activity throughout the entire heart. The ischemic/nonischemic ratio was 3:1 at 30 min.

Open-chested dogs were injected with BMS181321 following partial LAD occlusion and infusion of isoproterenol [67]. Uptake was seen in both planar and single-photon emission tomographic (SPET) images. Autoradiography revealed marked retention of activity in the LAD territory with an optical density ratio of 4:1 between the ischemic and nonischemic territories. Pronounced uptake was seen in the endo- and mesocardium, with little activity in the epicardium.

The myocardial kinetics of BMS-181321 in open-chested swine [72] was also studied in a model where flow through the LAD was reduced by 50%–80%. Initial planar imaging revealed a homogeneous distribution, but washout from normoxic tissue was more rapid ($T_{1/2}$ = 1.0±0.1 h) than that from the ischemic LAD territory ($T_{1/2}$ = 2.0±0.1 h), allowing visualisation of the LAD territory at the end of the reperfusion. Tissue activity of BMS-181321 was found to be inversely related to blood flow, as determined with microspheres.

### *Brain*

The direct cost of caring for patients with cerebral vascular disease was $17 billion in the United States in 1993 [73]. In additional $13 billion was spent on indirect costs, including patients' loss of productivity, bringing the total cost of cerebrovascular disease to $30 billion in 1993. Stroke affects approximately 550 000 people each year in the United States; more than 150 000 die. In patients with strokes, 73% are ischemic ($4 billion), 13% are hemorrhagic ($700 million), and 15% are transient ischemic attacks ($820 million). Management of stroke still remains largely expectant.

While function is impaired immediately when flow drops below a critical level, the development of morphological damage in the brain, as in the heart, depends upon some product of the severity of the flow reduction and the time. In the brain, the concept of the ischemic penumbra, an area of tissue subsequent to a stroke with flows below the functional threshold but above the threshold for morphological damage, is generally accepted [74] and is in keeping with the general understanding of the decrease in cell viability during ischemia. In the brain this tissue is vulnerable to subsequent damage independent of further external insults. Acute injury to the CNS causes glutamate and other excitatory amino acids (EAAs) to be released by damaged neurons, which induce an unregulated influx of calcium in surrounding neurons, resulting in cell death. There are believed to be four different EAA receptor subtypes and a number of different binding sites on the *N*-methyl-*D*-as-

partate (NMDA) receptor, including the NMDA recognition site, the ion channel site, and the polyamine site. Much effort is being expended to develop therapies that can protect this ischemic penumbra from the destruction caused by the progression of events after the initial stroke. It is likely that these drugs will have a small therapeutic index. The use of such drugs if and when they come into routine clinical use will depend upon both the identification of the type of stroke that is occurring/has occurred and the establishment of the presence of the jeopardized tissue in the ischemic penumbra. A hypoxic tissue imaging agent is well suited to this task because it will specifically identify tissue that is viable in an environment of diminished oxygen.

In vivo studies in experimental animals

Autoradiograms of brain from spontaneously hypertensive rats following middle cerebral artery occlusion (MCAO) show that BMS-181321 is selectively retained in acutely ischemic brain, but is not retained in infarction [75]. Double-label experiments comparing $^{14}$C-iodoantipyrine as a marker of perfusion to BMS-181321 revealed selective retention of BMS-181321 at the border of the ischemic zone. Evans Blue dye, a marker of blood-brain barrier integrity, was confined to the vasculature at this time. This result demonstrates that because of the high permeability of BMS-181321, its uptake is not dependent on disruption of the blood-brain barrier, as is true for X-ray and nuclear magnetic resonance contrast media. In contrast, at 24 h, BMS-181321 was not selectively retained in the now infarcted territory. This result is consistent with the fact that the enzymatic reduction required for trapping will not occur unless the cell is viable. Thus, this agent may prove useful for distinguishing between ischemic but viable and infarcted tissue, a distinction that is not possible with flow agents. Sequential SPET images of cat brain following MCAO demonstrated that the early distribution of BMS-181321 in images acquired between 2 and 8 min approximated blood flow, while images at 2.5 h showed preferential retention in the ischemic zone.

*Oncology*

In solid tumors experimental evidence suggests that if a significant fraction of tumor cells are hypoxic (the hypoxic fraction), the tumor has a higher malignant potential and a reduced sensitivity to radiation therapy and certain anticancer drugs. Recent results obtained with oxygen electrodes indicate considerable heterogeneity of oxygen levels in solid tumors, even for tumors of similar histology and size. However, in oxygen-electrode studies [76] that compared the survival rate and recurrence rate of advanced cervical cancer to local $pO_2$ levels in the cervix, a very strong correlation between low $pO_2$ and recurrence was noted. At a median follow-up of 19 months, in a group of 31 women, patients with a median intratumoral $pO_2$ ≤10 mmHg had a significantly lower survival and recurrence-free survival level than patients with tumors of >10 mmHg median $pO_2$. Nine of the ten patients with tumor progression or relapse had median $pO_2$ values of <10 mmHg. Tumor stage, size, histologic grading, and treatment modality were not significantly different between the two groups. Similar results were seen in an earlier study by Gatenby et al. [77] where the mean $pO_2$ in lymph node metastases in squamous cell carcinomas of the head and neck was correlated with tumor response to fractionated radiotherapy. Most (16/18) of the tumors with a mean $pO_2$ of 11–30 mmHg showed complete response to therapy. In contrast, 10/13 of the tumors with mean $pO_2$ values ≤10 mmHg showed no response to therapy. The heterogeneity of oxygen levels was not predicted by tumor histology or tumor volume. Unfortunately, oxygen-electrodes are invasive and technically complex to use, making them difficult to employ for routine clinical decision making. The noninvasive measurement of hypoxic fraction using radiolabeled nitroimidazoles may ultimately prove useful as a predictor of treatment outcome, or help to identify patients for therapies designed to overcome resistance to hypoxia.

In vitro

Biskupiak et al. [33] compared the anoxic to normoxic ratio of FMISO and IVM in a number of different tumor cell lines after 3 h of exposure (Table 3). In general the IVM gave a lower ratio than the FMISO. For both compounds there were some differences between the different cell lines.

Jette et al. [32] examined the retention of IAZR using EMT-6 cells. They found that the retention of 20 μ*M* IAZR by $10^6$ cells as measured by trichlor acetic acid precipitation increased linearly with time under hypoxic conditions and reached 16.7 times the normoxic value at 3 h, which is comparable to the figures for IVM and FMISO shown above. Over the concentration range of 10–100 μ*M* the initial rate of binding of IAZR exceeded that of MISO by 2–3 times. Mannan et al. [36] used the same systems and procedures to examine IAZA and found hypoxic to normoxic ratios of 17 at 3 h using 30 μ*M* IAZA.

**Table 3.** Mean anoxic to normoxic ratios after exposure for 3 h (from [33])

| Cell line | FMISO | IVM |
|---|---|---|
| RIF-1 | 28.5 | 23.2 |
| EMT-6 | 12.6 | 11.0 |
| V79 | 27.3 | 12.5 |
| CaOs-1 | 18.0 | 10.2 |

In vivo

Wiebe et al. [34] examined the uptake of IPENI in mice implanted with EMT-6 tumors. Although the maximum concentration in the tumor of 1.8% injected dose/g occurred at less than 1 h after injection, the long blood half-life of this compound kept the tumor to blood ratio at less than unity for the entire 72 h of the study. Parliament et al. [78] examined the uptake of IAZA in mice bearing EMT-6 or RIF-1 tumors. The drug was injected intraperitoneally at doses of 0.18, 1.8, and 18 mg/kg, which were chosen to give body concentrations of 0.5, 5.0, and 50 μ*M*. They found a linear increase in the amount of drug bound to the tumors after 24 h as the body concentration increased. There was little difference in the amount of material retained between the two tumor types; values ranged from 10 to 3000 n*M*/tumor. Wen et al. [79] have studied the binding of BMS-181321 to anoxic and normoxic L2981 tumor cells in vitro and found that the degree of binding increased with increased cell number, and rose as the temperature of the incubation medium was increased from 4°C to 37°C. Binding of BMS-181321 to anoxic cells was severalfold greater than that to normoxic cells. At 60 min, the hypoxic/normoxic (H/N) ratio at 37°C was 13.9:1. This ratio is similar to that obtained with the amido PnAO nitroimidazole reported recently [54]. When incubated with Chinese hamster V79 379A fibroblasts under hypoxic and normoxic conditions, the H/N ratio was reported to be 14.5:1, but only after 5 h of incubation. It is not clear how comparable these agents are, as absolute uptake values were not reported.

Moore et al. [80] explored the relationship between flow and retention of IAZA as a marker of hypoxia induced by photodynamic therapy (PDT). After PDT there is a general reduction in perfusion of the treated area caused by destruction of the tumor microvasulature. Tumor radioactivity increased with IAZA; however, there was no dependence on the light dose even though there is a relationship between light dose and efficacy. The IAZA tumor to brain ratios were 2.3 in the controls and 3.5 after PDT, an increase in signal of only 1.5 times. This contrasts with an increase in the signal of 2.4 times obtained by the same authors with MISO.

Mannan et al. [37] examined the uptake of IAZP in mice bearing EMT-6 tumors. The mice were injected intravenously with 0.3 mg (1 μmol) of material and sacrificed at various times up to 24 h post injection. The tumor levels remained at about 2% ID/g for 4 h over which time the tumor to blood ratio increased to about 5. This increased to 13.9 at 24 h (Table 4), although by this time the tumor levels had dropped by a factor of 4 from the 4-h levels. The optimum imaging time was thought to be 8–24 h post injection. The main route of excretion was the liver. Overall, the characteristics of IAZP were deemed to be superior to those of IAZR. The substitution of a hydroxyl group by a fluorine to give FIAZP.

**Table 4.** Tumor to blood ratios in mice implanted with EMT-6 tumors for iodinated sugars containing a 2-nitroimidazole group

| Compound | Log P | Blood at 24 h % ID/g | Deiodination | Tumor/blood at 24 h |
|---|---|---|---|---|
| MISO | –0.37 | 0.04 | O | 8.4 |
| IAZG | –0.24 | 0.06 | ++ | 1.4 |
| IAZP | –0.05 | 0.03 | + | 13.9 |
| IAZR | 0.32 | – | ++ | 5.5 |
| IAZA | 0.70 | 0.04 | ++ | 5.6 |
| FIAZP | 0.80 | 0.05 | + | 5.9 |

In vivo tissue distribution studies in nude mice with L2981 tumors indicated that BMS-181321 levels in the tumor remained constant at ~1% ID/g for 4 h, whereas the activity concentration in the contralateral hindflank was 0.2% ID/g. Microvascular $pO_2$ levels in these animals were determined using a technique [81, 82] based on the oxygen-dependent quenching of the phosphorescent lifetime of tetraphenyl porphine. Tumors had an average $pO_2$ of 3–5 Torr vs 14 Torr in the contralateral limb. Tumor uptake was also noted in C3H mice implanted with KHT, SCC VII, or RIF-1 murine tumors [83]. Absolute uptake was highest at 10 min, but tumor to muscle ratios increased with time, and plateaued at 4–8 h.

## Clinical studies

IAZA has been used in preliminary clinical studies to assess tumor hypoxia [84]. IAZA images were obtained in ten patients after intravenous injection of 6 mCi of $^{123}$I-IAZA over a 20-min period. The thyroid had previously been blocked with Lugol's solution. Immediate and 1-h images showed radioactivity in the liver, kidneys, and bladder together with radioactivity in the thyroid, salivary glands, etc. Blood clearance of the second phase had a $t_{1/2}$ of 9.8 h. Based upon the pharmacokinetics, in particular the blood clearance, the authors estimate that the best time to image the tumors is greater than 24 h post injection. The authors suggest that this could be earlier if blood clearance were faster. On later images the thyroid and salivary glands had increased uptake relative to the other organs. Uptake was seen in three of the ten tumors studied with tumor to adjacent normal tissue ratios of 3.1 at 16 h for a small cell lung carcinoma (SCLC) metastasis in the brain, 2.3 at 18 h for a primary SCLC, and 1.9 at 22 h for a malignant fibrous histiocytoma in the thigh. The second paper reported studies in 22 patients. 4–9 mCi of $^{123}$I-IAZA was injected initially over 10–20 min but subsequently as a bolus once no immediate toxic effects had been identified. The thyroid was blocked with Lugol's solution. Static planar imaging was performed up to 1 h after injection and SPET between 16 and 24 h after injection. HMPAO images were obtained within 1 week of the IAZA images. Of the 27 known tu-

mors, 13 showed increased uptake over adjacent normal tissue. Those tumors containing increased uptake of IAZA tended to have decreased uptake of HMPAO; however, glioblastoma multiforme showed no enhanced uptake of IAZA even in the presence of decreased HMPAO retention, i.e., low perfusion. Thus, the expected relationship between reduced flow and increased retention of a hypoxic tissue imaging agent does not appear to be a simple direct relationship and may vary with tumor type. As perfusion imaging is a surrogate for nutrient supply ($O_2$ measurements), one would expect the direct measurement of hypoxia to provide the better data.

*Stroke*

Several studies now suggest that many patients presenting with acute stroke have a peripheral zone of ischemic but viable tissue. Recent studies by Yeh et al. [85] in six patients with stroke studied within 2 h of the event demonstrated uptake of FMISO in three. A series of five patients with chronic stroke, on the other hand, did not concentrate FMISO in their lesions.

*Infection*

One of the earliest attempts to use nitroimidazoles for imaging was an effort to use radiolabeled METRO as an agent for imaging amebic hepatic abscesses [86]. Unfortunately, this effort produced equivocal results, and nitroimidazoles were not used again for imaging infection until 1994. Periodontal infections are frequently caused by anaerobic organisms, and are a common problem in the management of patients with head and neck cancer. Liu et al. [87] were able to identify almost half of clinically apparent periodontal disease in patients undergoing evaluation for head and neck cancer with FMISO imaging.

*Tumors*

In a series of 12 patients with head and neck tumors, on the other hand, all primary lesions and half of the 21 cervical nodal metastases were seen with FMISO imaging [88].

## Other methods for measuring oxygen in vivo

As the noninvasive measurement of tissue oxygen concentrations has such great potential, there have been various attempts to develop a method other than the radiopharmaceutical techniques described here.

An NMR active analogue of MISO labeled on the side chain with six fluorine atoms has been tested in EMT-6 tumors. The presence of $^{19}F$ was detected by NMR but there was evidence for substantial defluorination [89]. This is not surprising as the position of substitution is known to be cleaved in MISO. Further work was done with this and an additional compound, both of which were injected into mice at doses ranging from 0.25 to 3 mmol/kg (close to the toxic levels). NMR signals were seen in a variety of tumors as well as, of course, in the normoxic tissues [90]. Kwock et al. [91] compared the signal from the fluorinated MISO with the phosphocreatine/inorganic phosphate levels as determined by phosphorus-31 magnetic resonance spectroscopy (MRS) and the distribution of the compound as measured by immunohistochemistry. The existence of hypoxia was established by the $^{31}P$-MRS and the presence of the compound in the tissue by the immunohistochemistry; however, no $^{19}F$ signal could be detected at 24 h and the signal at earlier times was thought to be representative of perfusion rather than hypoxia. Others have also investigated the ability of antibodies to detect the nitroimidazoles and their conjugates in hypoxic tissue [92]. The relationship between the $^{31}P$-MRS measurement of hypoxia and the deposition of MISO has been measured [93]. Both techniques demonstrate marked variability in $pO_2$ levels in different tumors even in experimental animal studies but the reproducibility from day to day as measured by NMR is good.

A number of groups have used perfluorocarbon (PFC) emulsions as the oxygen-sensitive NMR visible signal. Mason et al. [94] performed spectroscopy on excised hearts after intravenous injection of the PFC and obtained a good relationship between the oxygen concentration and the NMR signal. Fast imaging allowed them to measure the $pO_2$ to an accuracy of ~20 Torr. They also performed imaging experiments; however, these took 19 h to acquire the necessary data set. Holland et al. [95] concentrated their efforts on the liver and spleen of rats in which the concentration of PFC is much higher than in the heart. As a result of the greater signal this provides they were able to measure $pO_2$ to within 7 Torr with a 13-min acquisition time. There is some doubt about the accuracy of the measurement as the values they obtained are 2 times those obtained using the well-accepted microelectrode methods. Some of the discrepancy might be related to the large amounts of PFC which are present in the tissue. Nevertheless, they could obtain images in approximately 1 h with a spatial resolution of 1–3 mm. Of some concern is the long half-life (10–70 days) of the PFCs used and also the 3–7 days of dosing that is required prior to imaging. Dardzinski and Sotak [96] have used a different PFC and echo-planar techniques to look at the liver, spleen, and tumors in mice. The values they have obtained for the $pO_2$ in the liver and spleen are in good agreement with the microelectrode studies. Images were obtained in 10–20 min. Lower resolution images can be obtained in 2.5 min in the tissues with high PFC concentration, such as the liver and spleen, and in 10 min in tumors. As yet these

NMR-based methods suffer from low spatial and/or temporal resolution and the need to administer large quantities of PFC which have long in vivo residence times.

Other alternatives to radiopharmaceuticals employed a fluorescent label [97, 98]. These appear to have promising properties for in vitro work but the limited range of the light wavelengths used may limit the usefulness in vivo.

## References


1. Guyton AC. Transport of oxygen and carbon dioxide in the blood and body fluids. In: Guyton DL, ed. *Textbook of physiology.* Philadelphia: W.B. Saunders; 1981: 504–515.
2. Berne RM, Levy MN. Skeletal physiology. In: Berne RM, Levy MN, eds. *Physiology, 3rd edn.* St. Louis: Mosby Yearbook; 1993: 292–308.
3. Berne RM, Levy MN. The peripheral circulation and its control. In: Berne RM, Levy MN, eds. *Physiology, 3rd edn.* St. Louis: Mosby Yearbook; 1993: 478–493.
4. Liu P, Kiess MC, Okada RD, Block PC, Strauss HW, Pohost GM, Boucher CA. The persistent defect on exercise thallium imaging and its fate after myocardial revascularization: Does it represent scar or ischemia? *Am Heart J* 1985; 110: 996–1001.
5. Straub NC. Transport of oxygen and carbon dioxide: tissue oxygenation. In: Berne RM, Levy MN, eds. *Physiology, 3rd edn.* St. Louis: Mosby Yearbook; 1993: 590–598.
6. Buxton RB, Alpert NM, Babikian V, Weise S, Correia JA, Ackerman RH. Evaluation of the $^{11}CO_2$ positron emission tomographic method for measuring brain pH. I. pH changes measured in states of altered $PCO_2$. *J Cereb Blood Flow Metab* 1987; 6: 709–719.
7. Olive PL, Durand RE. Misonidazole binding in SCCVII tumors in relation to the tumor blood supply. *Int J Radiat Oncol Biol Phys* 1989; 16: 755–761.
8. Connet RJ, Honig CG, Gayeski E, Brooks GA. Defining hypoxia: a systems view of $VO_2$, glycolysis, energetics and intercellular $PO_2$. *J Appl Physiol* 1990; 68: 833–842.
9. Cotran RS, Kumar V, Robbins SL. Cellular injury and adaption. In: Cotran RS, Kumar V, Robbins SL, eds. *Robbins pathologic basis of disease, 4th edn.* Philadelphia: W.B. Saunders; 1989: 1–38.
10. Webster LT. Drugs used in chemotherapy of protozoal infections. In: Gilman AG, Rall TW, Nies AS, Taylor P, eds. *The pharmacological basis of therapeutics, 8th edn.* New York: Pergamon; 1990: 1002–1004.
11. Edwards DI. Nitroimidazole drugs – action and resistance mechanisms. 1. Mechanisms of action. *J Antimicrob Chemother* 1993; 31: 9–20.
12. Brown JM. Hypoxic cell radiosensitisers: Where next? *Int J Radiat Oncol Biol Phys* 1989; 16: 987–993.
13. Chapman JD, Franko AJ, Sharplin J. A marker for hypoxic cells in tumours with potential clinical applicability. *Br J Cancer* 1981; 43: 546–550.
14. Kedderris GL, Miwa GT. The metabolic activation of nitroheterocyclic therapeutic agents. *Drug Metab Rev* 1988; 19: 33–62.
15. de Jong JW, van der Meer P, Nieukoop AS, Huizer T, Stroeve RJ, Bos E. Xanthine oxidoreductase activity in perfused hearts of various species, including humans. *Circ Res* 1990; 67: 770–773.
16. Bolton JL. McClellan RA. Kinetics and mechanism of the decomposition in aqueous solutions of 2-(hydroxyamino)imidazoles. *J Am Chem Soc* 1989; 111: 8172–8181.
17. Varghese AJ, Whitmore GF. Properties of 2-hydroxylaminoimidazoles and their implications for the biological effects of 2-nitroimidazoles. *Chem Biol Interact* 1985; 56: 269–287.
18. Adams GE, Clarke ED, Flockhart IR, Jacobs RS, Sehmi DS, Stratford IJ, Wardman P, Watts ME, Parrick J, Wallace RG, Smithen CE. Structure-activity relationships in the development of hypoxic cell radiosensitisers. I. Sensitisation efficiency. *Int J Radiat Biol* 1979; 35: 133–150.
19. White RAS, Workman P, Brown JM. The pharmacokinetics and tumour and neural tissue penetrating properties of SR-2508 and SR-2555 in the dog – hydrophilic radiosensitisers potentially less toxic than misonidazole. *Radiat Res* 1980; 84: 542–561.
20. Sasai K, Iwai H, Yoshizawa T, Nishimoto S, Shibamoto Y, Kitakabu Y, Oya N, Takahashi M, Abe M. Pharmacokinetics of fluorinated 2- nitroimidazole hypoxic cell radiosensitisers in murine peripheral nervous tissue. *Int J Radiat Biol* 1992; 62: 221–227.
21. Workman P, Brown JM. Structure-pharmacokinetic relationships for misonidazole analogues in mice. *Cancer Chemother Pharmacol* 1981; 6: 39–49.
22. Chin JB, Rauth AM. The metabolism and pharmacokinetics of the hypoxic cell radiosensitiser and cytotoxic agent, misonidazole in C3H mice. *Radiat Res* 1981; 86: 341–357.
23. Grunbaum Z, Freauff SJ, Krohn KA, Wilbur DS, Magee S, Rasey JS. Synthesis and characterisation of congeners of misonidazole for imaging hypoxia. *J Nucl Med* 1987; 28: 68–75.
24. Vanderkooi JM, Erecinska M, Silver IA. Oxygen in mammalian tissue: methods of measurement and affinities of various reactions. *Am J Physiol* 260: C1131–C1150.
25. Roizin-Towle L, Hall EJ, Pirro JP. Oxygen dependence for chemosensitisation by misonidazole. *Br J Cancer* 1986; 54: 919–924.
26. Olive PL, Durand RE. Misonidazole binding in SCCVII tumours in relation to the tumour blood supply. *Int J Radiat Oncol Biol Phys* 1989; 16: 755–761.
27. Urtasun RC, Chapman JD, Raleigh JA, Franko AJ, Koch CJ. Binding of $^{3}H$-misonidazole to solid human tumours as a measure of tumour hypoxia. *Int J Radiat Oncol Biol Phys* 1986; 12: 1263–1267.
28. Hoffman JM, Rasey JS, Spence AM, Shaw DW, Krohn KA. Binding of the hypoxia tracer [$^{3}H$]misonidazole in cerebral ischaemia. *Stroke* 1987; 18: 168–176.
29. Garrecht BM, Chapman JD. The labeling of EMT-6 tumors in BALB/C mice with $^{14}C$-misonidazole. *Br J Radiol* 1983; 56: 745–753.
30. Blasberg R, Horowitz M, Strong J, Molnar P, Patlak C, Owens E, Fenstermacher J. Regional measurements of [$^{14}C$]misonidazole distribution and blood flow in subcutaneous RT-9 experimental tumours. *Cancer Res* 1985; 45: 1692–1701.
31. Rasey JS, Krohn KS, Freauff S. Bromomisonidazole: synthesis and characterisation of a new radiosensitiser. *Radiat Res* 1982; 91: 542–554.
32. Jette DC, Wiebe LI, Chapman JD. Synthesis and in vivo studies of the radiosensitiser 4-[$^{82}Br$]bromomisonidazole. *Int J Nucl Med Biol* 1983; 10: 205–210.
33. Biskupiak JE, Grierson JR, Rasey JS, Martin GV, Krohn KA. Synethesis of an (iodovinyl)misonidazole derivative for hypoxia imaging. *J Med Chem* 1991; 34: 2165–2168.
34. Wiebe LI, Jette DC, Chapman JD. Electron-affinic compounds for labelling hypoxic cells: the synthesis and characterisation

of 1-[2-([2-iodophenoxy)ethyl]-2-nitroimidazole. *Nuklearmedizin* 1984; 23: 63–67.
35. Jette DC, Wiebe LI, Lee J, Chapman JD. Iododoazomycin riboside (1-(5'-iodo-5'-deoxyribofuranosyl)-2-nitroimidazole), a hypoxic cell marker. 1. Synthesis and in-vitro characterization. *Radiat Res* 1986; 105: 169–179.
36. Mannan RH, Somayaji VV, Lee J, Mercer JR, Chapman JD, Wiebe LI. Radioiodinated 1-(5-iodo-5'-deoxy-D-arabinofuranosyl)-2-nitroimidazole (iodoazomycin arabinoside: IAZA); a novel marker of tissue hypoxia. *J Nucl Med* 1991; 32: 1764–1770.
37. Mannan RH, Mercer JR, Wiebe LI, Kumar P, Saomayaji VV, Chapman JD. Radioiodinated azomysin pyranoside (IAZP): a novel noninvasive marker for the assessment of tumor hypoxia. *J Nucl Med Biol* 1992; 36: 60–67.
38. Mannan RH, Mercer JR, Weibe LI, Samayaji VV, Chapman JD. Radioiodinated 1-(2-fluoro-4-iodo-2,3-dideoxy—L-xylopyranosyl)-2-nitroimidazole: a novel probe for the noninvasive assessment of tumor hypoxia. *Radiat Res* 1992; 132: 368–374.
39. Jerabek PA, Dischino DD, Kilborn MR, Welch MJ. Synthesis of a fluorine-18 labeled hypoxic cell sensitizer [abstract]. *J Nucl Med* 1984; 25: P23.
40. Jerabeck PA, Patrick TB, Kilbourn MR, et al. Synthesis and biodistribution of $^{18}$F-labeled fluoronitroimidazoles: potential in vivo markers of hypoxic tissue. *Int J Radiat Appl Instrum [A]* 1986; 37: 599–605.
41. Grierson JR, Link JM, Mathis CA, Rasey JS, Krohn KA. A radiosynthesis of fluorine-18 fluoromisonidazole. *J Nucl Med* 1989; 30: 343–350.
42. Rasey JS, Grunbaum Z, Magee S, Nelson NJ, Olive PL, Durand RE, Krohn KA. Characterization of radiolabeled fluoromisonidazole as a probe for hypoxic cells. *Radiat Res* 1987; 111: 292–304.
43. Rasey JS, Koh W-J, Grierson JR, Grunbaum Z, Krohn KA. Radiolabeled fluoromisonidazole as an imaging agent for tumor hypoxia. *Int J Radiat Oncol Biol Phys* 1989; 17: 985–991.
44. Martin GV, Caldwell JC, Rasey JS, Grunbaum Z, Cerqueira M, Krohn KA. Enhanced binding of the hypoxic cell marker [H-3]-fluoromisonidazole in ischemic myocardium. *J Nucl Med* 1989; 30: 194–201.
45. Linder KE, Chan YW, Cyr JE, Nowotnik DP, Eckelman WC, Nunn AD. Synthesis, characterization and in vitro evaluation of nitroimidazole-BATO complexes: new technetium compounds designed for imaging hypoxic tissue. *Bioconj Chem* 1993; 4: 326–333.
46. Raju N, Ramalingam K, Nowotnik DP. Synthesis of some nitroimidazole boronic acids: precursors to technetium-99m complexes with potential for imaging hypoxic tissue. *Tetrahedron* 1993; 48: 10233–10238.
47. Clarke ED, Wardman P, Goulding KH. Anaerobic reduction of nitroimidazoles by reduced flavin mononucleotide and xanthine oxidase. *Biochem Pharmacol* 1980; 329: 2684–2687.
48. Josephy PD, Palcic B, Skarsgard LD. Reduction of misonidazole and its derivatives by xanthine oxidase. *Biochem Pharmacol* 1981; 31: 3237–3242.
49. Predegas JL, Rasey JS, Grunbaum Z, Krohn K. Reduction of fluoromisonidazole and its derivatives by xanthine oxidase. *Biochem Pharmacol* 1991; 42: 2387–2395.
50. Linder KE, Chan YW, Cyr JE, Malley MF, Nowotnik DP, Nunn AD. $^{99}$TcO(PnAO-1-2-nitroimidazole) [BMS-181321], a new technetium-containing nitroimidazole complex for imaging hypoxia: synthesis, characterization and xanthine oxidase-catalyzed reduction. *J Med Chem* 1994; 37: 9–17.
51. Pirro JP, Di Rocco RJ, Narra RK, Nunn AD. The relationship between in-vitro trans-endothelial permeabilty and in-vivo single-pass brain extraction of several SPECT imaging agents. *J Nucl Med* 1994; In press.
52. Linder KE, Cyr JE, Chan Y-W, Raju N, Ramalingam K, Nanjappan P, Nowotnik D, Wedeking P, Rumsey W, Narra RK, Nunn AD. Effect of substituents on physiochemical and biological behavior of Tc-Pnao nitroimidazoles [abstract]. *J Nucl Med* 1994; 35: 18P.
53. Chan Y-W, Romero V, Linder KE, Patel BC, Jayatilak PG, Nunn AD, Rumsey W. In-vitro studies on the hypoxia retention of a novel technetium-99m labeled nitroimidazole in rat heart [abstract]. *J Nucl Med* 1994; 35: 152P.
54. New radiolabeled diamino mono- and dioximino compounds – useful for treating tumors and as imaging agents in diagnostics. World Patent Appl. WO94089-A1, Amersham Int. plc.
55. Neumeier R, Kramp W, Macke H. Chelating agents for forming complexes with radioactive isotopes, metal complexes thereof and use thereof in diagnosis and therapy. Eur Patent Appl 0417870 A2. 1990.
56. Ramalingam K, Raju N, Nanjappan P, Linder KE, Pirro J, Zeng W, Rumsey W, Nowotnik DP, Nunn AD. The synthesis and in vitro evaluation of a $^{99m}$Tc nitroimidazole complex based on a bis(amine-phenol) ligand. Comparison to BMS 18134. *J Med Chem;* In press.
57. Sapirstein LA. Regional blood flow by the fractional distribution of indicators. *Am J Physiol* 1958; 193: 161–168.
58. Famighetti R, Funk, Wagnalls, Mahwah NJ, eds. *The world almanac and book of facts*. 1994: 691.
59. Berne RM, Levy MN. Special circulations. In: Berne RM, Levy MN, eds. *Physiology, 3rd edn.* St. Louis: Mosby Yearbook; 1993: Chap. 31.
60. Uren NG, Crake T, Lefroy DC, de Silva R, Davies GJ, Maseri A. Reduced coronary vasodilator function in infarcted and normal myocardium after myocardial infarction. *N Engl J Med* 1994; 331: 222–227.
61. Braunwald E, Sobel BE. Coronary flow and myocardial ischemia. In: Barunwald E, ed. *Heart Disease, 4th edn.* Philadelphia: W.B. Saunders; 1992: 1161–1191.
62. Opie-LH. The mechanism of myocyte death in ischaemia. *Eur Heart J* 1993; 14 Suppl G: P 31–33.
63. Wynne J, Holman BL. Acute myocardial infarct scintigraphy with infarct-avid radiotracers. *Med Clin North Am* 1980; 64: 119–144.
64. Rumsey WL, Patel B, Kuczynski B, Narra RK, Chan YW, Linder KE, Cyr J, Raju N, Ramalingam K, Nunn AD. Potential of nitroimidazoles as markers of hypoxia in heart. In: Vaupel P et al., eds. *Oxygen transport to tissue*. New York: Plenum; 1994: 263–270.
65. Shelton ME, Dence CS, Hwang DR, Welch MJ, Bergmann SR. Myocardial kinetics of fluorine 18 misonidazole: a marker of hypoxic myocardium: *J Nucl Med* 1989; 30: 351–358.
66. Rumsey WL, Cyr JE, Raju N, Narra RK. A novel [99m]technetium-labeled nitroheterocycle capable of identification of hypoxia in heart. *Biochem Biophys Res Commun* 1993; 193: 1239–1246.
67. Rumsey WL, Patel B, Linder KE. The effect of graded hypoxia on the retention of a novel $^{99m}$Tc-nitroheterocycle in the perfused rat heart. *J Nucl Med* 1994; In press.
68. Kusuoka H, Hashimoto K, Fukuchi K, Nishimura T. Kinetics of a putative hypoxic tissue marker, technetium-99m-nitroim-

idazole (BMS-181321), in normoxic, hypoxic, ischemic and stunned myocardium, *J Nucl Med* 1994; 35: In press.
69. Martin GV, Biskupiak JE, Caldwell JH, Rasey JS, Krohn KA. Characterization of iodovinylmisonidazole as a marker for myocardial hypoxia. *J Nucl Med* 1993; 34: 918–923.
70. Goldstein RA. Wanted dead or alive – the search for markers of myocardial viability. *J Am Coll Cardiol* 1990; 16: 486–488.
71. Di Rocco RJ, Bauer A, Kuczynski BL, Pirro JP, Linder KE, Narra RK, Nunn AD. Imaging regional hypoxia with a new technetium-labeled imaging agent in rabbit myocardium after occlusion of the left anterior descending coronary artery [abstract]. *J Nucl Med* 1992; 33: 865.
72. Stone CK, Mulnix T, Nickles RJ, Renstrom B, Nellis SH, Liedtke AJ, Nunn AD. Myocardial kinetics of a putative hypoxic tissue marker. Technetium-99m-labeled nitroimidazole (BMS-181321) after regional ischemia and reperfusion [abstract]. *J Nucl Med* 34: 16P.
73. Matchar D. Pink sheet. 23 May 1993.
74. Heiss WD. Flow thresholds of functional and morphological damage of brain tissue. *Stroke* 1983; 14: 329–331.
75. Di Rocco RJ, Kuczynski BL, Pirro JP, Bauer A, Linder KE, Ramalingam K, Cyr JE, Chan Y-W, Raju N, Narra RK, Nowotnik DP, Nunn AD. Imaging ischemic tissue at risk of infarction during stroke. *J Cereb Blood Flow Metab* 1993; 13: 755–762.
76. Hockel M, Knoop C, Schlenger K, Vorndran B, Knapstein PG, Vaupel P. Intratumoral $pO_2$ histography as predictive assay in advanced cancer of the uterine cervix. In: Vaupel P et al., eds. *Oxygen transport to tissue XV*. New York: Plenum; 1994: 445–450.
77. Gatenby RA, Kessler HB, Rosenblum JS, Coia LR, Moldofsky PJ, Hartz WH, Broder GJ. Oxygen distribution in squamous cell carcinoma metastases and its relationship in outcome of radiation therapy. *Int J Radiat Oncol Biol Phys* 1988; 14: 831–838.
78. Parliament MB, Chapman JD, Urtasun RC, McEwan AL, Golberg L, Mercer JR, Mannan RH, Weibe LI. Noninvasive assessment of human tumor hypoxia with $^{123}$I-iodoazomycin arabinoside: preliminary report of a clinical study. *Br J Cancer* 1992; 65: 90–95.
79. Wen M, Jayatilak PG, Bauer A, Patel B, Rumsey WL. Potential of a novel hypoxia agent BMS-181321 as a tumor marker. Proc. of 42nd annual meeting of the Radiation Research Society, Nashville, Tenn., 29 April–4 May 1994. p 249 [abstract].
80. Moore RB, Chapman JD, Mercer JR, Mannan R, Wiebe LI, McEwan A, McPhee S. Measurement of PDT-induced hypoxia in Dunning prostate tumors by iodine-123-*p*-iodoazomycin arabinoside. *J Nucl Med* 1993; 34: 405–413.
81. Wilson DF, Rumsey WL, Green TJ, Vanderkooi JM. The oxygen dependence of mitochondrial oxidative phosphorylation measured by a new optical method for measuring oxygen concentration. *J Biol Chem* 1988; 263: 2712.
82. Rumsey WL, Patel B, Kuczynski B, Bauer A. Phosphorescence quenching and technetium-linked nitroimidazoles: two new methods for detection of hypoxia in heart. *Adv Exp Med Biol* 1994; In press.
83. Ballinger JR, Wan Min Kee J, Rauth AM. In vitro and in vivo studies of a technetium-99m labelled 2-nitroimidazole derivative. Proc. of 42nd annual meeting of the Radiation Research Society, Nashville, Tenn. 29 April-4 May 1994. p 145 [abstract].
84. Groshar D, McEwan AJB, Parliament MB, Urtashun RC, Golberg LE, Hoskinson M, Mercer JR, Mannan RH, Weibe LI, Chapman JD. Imaging tumor hypoxia and tumor pefusion. *J Nucl Med* 1993; 34: 885–888.
85. Yeh SH, Liu RS, Hu HH, Chang CP, Chu LS, Chou KL, Wu LC. Ischemic penumbra in acute stroke: demonstration by PET with fluorine-18 fluoromisonidazole [abstract]. *J Nucl Med* 1994; 35: 205P.
86. Tubis M, Krishnamurthy G, Endow JS, Stein RA, Suwanik R, Blahd WH. Labeled metronidazoles as potential agents for amebic hepatic abscess imaging. *J Nucl Med* 1975; 14: 163–171.
87. Liu RS, Yeh SH, Chang CP, Chu LS, Lui MT, Chou KL, Yu LC. Detection of odontogenic infections by F-18 fluoromisonidazole (FMISO) [abstract]. *J Nucl Med* 1994; 35: 113P.
88. Yeh SH, Wu LC, Liu RS, Yang DJ, Yen SH, Yu TW, Chang CW, Chen KY. Fluorine-18 fluoromisonidazole (F-18-MISO) tumor: muscle retention ratio in detecting hypoxia in nasopharyngeal carcinoma [abstract]. *J Nucl Med* 1994; 35: 142P.
89. Raleigh JA, Franko AJ, Treiber EO, Lunt JA, Allen PS. Covalent binding of fluorinated 2-nitroimidazole to EMT-6 tumours in Balb/C mice. Detection by F-19 nuclear magnetic resonance at 2.35 T. *Int J Radiat Oncol Biol Phys* 1986; 12: 1249–1251.
90. Maxwell RJ, Workman P, Griffiths JR. Demonstration of tumour-selective retention of fluorinated nitroimidazole probes by 19F magnetic resonance spectroscopy in vivo. *Int J Radiat Oncol Biol Phys* 1989; 16: 925–929.
91. Kwock L, Gill M, McMurray HL, Beckman W, Raleigh JA, Joseph AP. Evaluation of a fluorinated 2-nitroimidazole binding to hypoxic cells in tumour-bearing rats by 19F magnetic resonance spectroscopy and immunohistochemistry. *Radiat Res* 1992; 129: 71–78.
92. Koch CJ, Lord EM. Detection of hypoxia. International patent application WO 94/11348. 1994
93. Chapman JD, McPhee MS, Walz N, Chetner MP, Stobbe CC, Soderlind K, Arnfield M, Meeker BE, Trimble L, Allen PS. Nuclear magnetic resonance spectroscopy and sensitiser-adduct measurements of photodynamic therapy-induced ischaemia in solid tumours. *J Natl Cancer Inst* 1991; 83: 1650-1659.
94. Mason RP, Jeffrey FMH, Malloy CR, Babcock EE, Antich PP. A noninvasive assessment of myocardial oxygen tension; 19F NMR spectroscopy of sequestered perfluorocarbon emulsion. *Magn Reson Med* 1992; 27; 27: 310–317.
95. Holland SK, Kennan RP, Schaub MM, D'Angelo MJ, Gore JC. Imaging oxygen tension in liver and spleen by 19F NMR. *Magn Reson Med* 1993; 29: 446–458.
96. Dardzinski BJ, Sotak CH. Rapid tissue oxygen tension mapping using 19F inversion-recovery echo-planar imaging of perfluoro-15-crown-5-ether. *Magn Reson Med* 1994; 32: 88–97.
97. Hodgkiss RJ, Jones GW, Long A, Middleton RW, Parrick J, Stratford MRL, Wardman P, Wilson GD. Fluorescent markers for hypoxic cells: a study of nitroaromatic compounds with fluorescent heterocyclic side chains, that undergo bioreductive binding. *J Med Chem* 1991; 34: 2268-2274.
98. Hodgkiss RJ, Begg AC, Middleton RW, Parrick J, Stratford MRL, Wardman P, Wilson GD. Fluorescent markers for hypoxic cells. A study of novel heterocyclic compounds that undergo bioreductive binding. *Biochem Pharmacol* 1991; 41: 533–541.